

# CAST constraints on the axion-electron coupling

K. Barth,<sup>a</sup> A. Belov,<sup>b</sup> B. Beltran,<sup>c,2</sup> H. Bräuninger,<sup>d</sup>  
 J. M. Carmona,<sup>c</sup> J. I. Collar,<sup>e</sup> T. Dafni,<sup>c,j,f</sup> M. Davenport,<sup>a</sup>  
 L. Di Lella,<sup>a,3</sup> C. Eleftheriadis,<sup>g</sup> J. Englhauser,<sup>d</sup> G. Fanourakis,<sup>h</sup>  
 E. Ferrer-Ribas,<sup>j</sup> H. Fischer,<sup>k</sup> J. Franz,<sup>k</sup> P. Friedrich,<sup>d</sup> J. Galán,<sup>c,j</sup>  
 J. A. García,<sup>c</sup> T. Geralis,<sup>h</sup> I. Giomataris,<sup>j</sup> S. Gninenko,<sup>b</sup>  
 H. Gómez,<sup>c,4</sup> M. D. Hasinoff,<sup>l</sup> F. H. Heinsius,<sup>k,5</sup>  
 D. H. H. Hoffmann,<sup>f</sup> I. G. Irastorza,<sup>c,a,j</sup> J. Jacoby,<sup>m</sup> K. Jakovčić,<sup>n</sup>  
 D. Kang,<sup>k,6</sup> K. Königsmann,<sup>k</sup> R. Kotthaus,<sup>o</sup> K. Kousouris,<sup>h,7</sup>  
 M. Krčmar,<sup>n</sup> M. Kuster,<sup>d,f,8</sup> B. Lakić,<sup>n</sup> A. Liolios,<sup>g</sup> A. Ljubičić,<sup>n</sup>  
 G. Lutz,<sup>p,9</sup> G. Luzón,<sup>c</sup> D. W. Miller,<sup>e</sup> T. Papaevangelou,<sup>a,j</sup>  
 M. J. Pivovarov,<sup>q</sup> G. Raffelt,<sup>o</sup> J. Redondo,<sup>o,r</sup> H. Riege,<sup>f</sup>  
 A. Rodríguez,<sup>c</sup> J. Ruz,<sup>q,a,c</sup> I. Savvidis,<sup>g</sup> Y. Semertzidis,<sup>s</sup>  
 L. Stewart,<sup>a</sup> K. Van Bibber,<sup>q,10</sup> J. D. Vieira,<sup>e,11</sup> J. A. Villar,<sup>c</sup>  
 J. K. Vogel,<sup>q,k</sup> L. Walckiers,<sup>a</sup> K. Zioutas<sup>f,a,t</sup>

<sup>a</sup>European Organization for Nuclear Research (CERN), Genève, Switzerland

<sup>b</sup>Institute for Nuclear Research (INR), Russian Academy of Sciences, Moscow, Russia

<sup>c</sup>Laboratorio de Física Nuclear y Altas Energías, Universidad de Zaragoza, Zaragoza, Spain

<sup>d</sup>Max-Planck-Institut für extraterrestrische Physik, Garching, Germany

<sup>e</sup>Enrico Fermi Institute and KICP, University of Chicago, Chicago, IL, USA

<sup>f</sup>Technische Universität Darmstadt, IKP, Darmstadt, Germany

<sup>g</sup>Aristoteles University of Thessaloniki, Thessaloniki, Greece

<sup>h</sup>National Center for Scientific Research “Demokritos”, Athens, Greece

<sup>j</sup>IRFU, Centre d’Études Nucléaires de Saclay (CEA-Saclay), Gif-sur-Yvette, France

---

<sup>1</sup>Present address: Institute de Physique Nucléaire, Lyon, France

<sup>2</sup>Present address: Department of Physics, Queens University, Kingston, Ontario

<sup>3</sup>Present address: Sezione di Pisa, IT

<sup>4</sup>Present address: Laboratoire de l’Accélérateur Linéaire, Centre Scientifique d’Orsay, 91898 Orsay, France

<sup>5</sup>Present address: Institut für Experimentalphysik, Ruhr-Universität Bochum, Bochum, Germany

<sup>6</sup>Present address: Karlsruhe Institute of Technology, Germany

<sup>7</sup>Present address: European Organization for Nuclear Research (CERN), Genève, Switzerland

<sup>8</sup>Present address: European XFEL GmbH, Notkestrasse 85, 22607 Hamburg, Germany

<sup>9</sup>Present address: PNSensor GmbH, München, Germany

<sup>10</sup>Present address: Department of Nuclear Engineering, University of California Berkeley, USA

<sup>11</sup>Present address: California Institute of Technology, USA

<sup>k</sup>Albert-Ludwigs-Universität Freiburg, Freiburg, Germany

<sup>l</sup>Department of Physics and Astronomy, University of British Columbia, Vancouver, Canada

<sup>m</sup>J. W. Goethe-Universität, Institut für Angewandte Physik, Frankfurt am Main, Germany

<sup>n</sup>Rudjer Bošković Institute, Zagreb, Croatia

<sup>o</sup>Max-Planck-Institut für Physik, Munich, Germany

<sup>p</sup>MPI Halbleiterlabor, München, Germany

<sup>q</sup>Lawrence Livermore National Laboratory, Livermore, CA, USA

<sup>r</sup>Arnold Sommerfeld Center, Ludwig-Maximilians-Universität, Munich, Germany

<sup>s</sup>Brookhaven National Laboratory, Brookhaven, USA

<sup>t</sup>Physics Department, University of Patras, Patras, Greece

E-mail: [Jaime.Ruz@cern.ch](mailto:Jaime.Ruz@cern.ch), [Julia.Vogel@cern.ch](mailto:Julia.Vogel@cern.ch), [redondo@mpp.mpg.de](mailto:redondo@mpp.mpg.de)

**Abstract.** In non-hadronic axion models, which have a tree-level axion-electron interaction, the Sun produces a strong axion flux by bremsstrahlung, Compton scattering, and axio-recombination, the “BCA processes.” Based on a new calculation of this flux, including for the first time axio-recombination, we derive limits on the axion-electron Yukawa coupling  $g_{ae}$  and axion-photon interaction strength  $g_{a\gamma}$  using the CAST phase-I data (vacuum phase). For  $m_a \lesssim 10$  meV/ $c^2$  we find  $g_{a\gamma} g_{ae} < 8.1 \times 10^{-23}$  GeV $^{-1}$  at 95% CL. We stress that a next-generation axion helioscope such as the proposed IAXO could push this sensitivity into a range beyond stellar energy-loss limits and test the hypothesis that white-dwarf cooling is dominated by axion emission.

**Keywords:** axions, helioscopes, sun, magnetic fields, white dwarfs

**ArXiv ePrint:** [1302.6283](https://arxiv.org/abs/1302.6283)

---

## Contents

|          |  |           |
|----------|--|-----------|
| <b>1</b> | <b>Introduction and main results</b>                 | <b>1</b>  |
| <b>2</b> | <b>Properties of axions and axion-like particles</b> | <b>5</b>  |
| <b>3</b> | <b>Expected counting rate</b>                        | <b>6</b>  |
| 3.1      | Solar flux   | 6         |
| 3.2      | Helioscope event number                              | 7         |
| <b>4</b> | <b>CAST experiment and analysis</b>                  | <b>7</b>  |
| 4.1      | The X-ray telescope of CAST                          | 8         |
| 4.2      | Data taking  | 8         |
| 4.3      | Spectral fitting results                             | 9         |
| 4.4      | Systematic uncertainties                             | 10        |
| <b>5</b> | <b>Conclusions</b>                                   | <b>10</b> |

---

## 1 Introduction and main results

The CERN Axion Solar Telescope (CAST) [1] is a helioscope experiment aiming at the detection of axions and axion-like particles (ALPs) emitted from the Sun. The detection principle is based on the axion<sup>1</sup> coupling to two photons, which triggers their conversion into photons of the same energy as they propagate through a transverse magnetic field [2, 3]. CAST has tracked the Sun in three different campaigns (2003–04 [4, 5], 2005–2006 [6] and 2008 [7]) with a 9.26 m long, 9 Tesla strong, decommissioned LHC dipole test magnet while measuring the flux of X-rays at the exits of both bores with four different low-background detectors. No excess counts were observed over the expected backgrounds, thus constraining the axion parameters, notably mass and couplings to photons [4–7] and nucleons [8, 9]. Such constraints require knowledge of the flux of axions emitted from the Sun which can be computed very precisely because the solar interior is a tractable weakly-coupled plasma.

The physics case of CAST was mainly focused on hadronic axions [10, 11] which were appealing as hot dark matter candidates [12]. Hadronic axion models are minimal in that the generic axion interactions with hadrons and photons derive from mixing with the pseudoscalar mesons  $\pi^0$ ,  $\eta$  and  $\eta'$ . The interactions with leptons arise at loop level [13] and are usually irrelevant. In hadronic models, the bulk of the solar axion flux comes from Primakoff production  $\gamma + Q \rightarrow a + Q$  [14–16], where  $Q$  is any charged particle.

Recently, non-minimal axion models are receiving increasing attention [17–26]. From the theoretical point of view, axions are nowadays known to arise naturally in many extensions of the standard model that pursue some sort of unification, such as Grand Unified Theories or string theory. Indeed, the original hadronic KSVZ axion [10, 11] can be regarded as an exemplary toy model that contains only the essential ingredients to solve the strong CP problem [27], but often axions arising in completions of the standard model are not minimal in this sense.

---

<sup>1</sup>Unless otherwise noted, the term “axion” henceforth includes both QCD axions and more general ALPs.

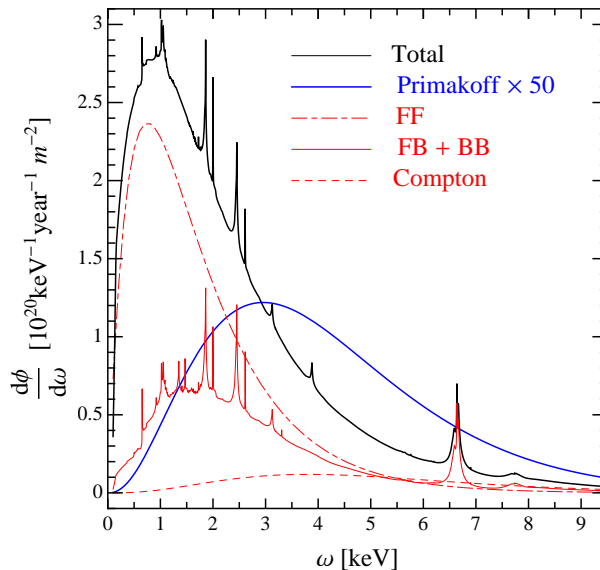


**Figure 1.** Solar axion flux on Earth for a typical DFSZ model with interaction strength to photons  $g_{a\gamma} = 10^{-12} \text{ GeV}^{-1}$  and electrons  $g_{ae} = 10^{-13}$ , corresponding to  $f_a = 0.85 \times 10^9 \text{ GeV}$  [30]. The blue line corresponds to the Primakoff flux and the red lines show the different components of the BCA flux: FF = free-free (bremsstrahlung), FB = free-bound (axio-recombination), and BB = bound-bound (axio-deexcitation). The black line is the total flux.

Non-hadronic axion models such as that of DFSZ [28, 29] have different and very interesting phenomenological consequences. Notably, they couple to electrons at tree level, and this opens axion-production channels in stars which are much more effective than the Primakoff process: electron-ion bremsstrahlung ( $e + I \rightarrow e + I + a$ ) [15, 31], electron-electron bremsstrahlung ( $e + e \rightarrow e + e + a$ ) [15], Compton ( $\gamma + e \rightarrow e + a$ ) [32, 33], axio-recombination ( $e + I \rightarrow I^- + a$ ) [30, 34–36] and, to a lesser extent, axio-deexcitation of ions ( $I^* \rightarrow I + a$ ). Henceforth we shall refer to this set of reactions as BCA for its most relevant contributions from bremsstrahlung, Compton, and axio-recombination. Indeed, axions with  $g_{ae} \sim 10^{-13}$  might explain the longstanding anomaly in the cooling of white dwarfs (WD) [37], recently reinforced by updated studies of the period decrease of the pulsating white dwarfs G117-B15A [38, 39] and R548 [40] and the WD luminosity function [41–44]. One should note that this value is somewhat challenged by the constraint  $g_{ae} < 2.5 \times 10^{-13}$  imposed by the evolution of red giant stars in globular clusters [45, 46]. These values of  $g_{ae}$  imply a DFSZ-axion decay constant  $f_a \sim 10^9 \text{ GeV}$  (corresponding to an axion mass  $m_a \sim \text{meV}$ ). Such meV-mass axions have a wealth of other interesting phenomenological implications in the context of astrophysics, like the formation of a cosmic diffuse background of axions from core collapse supernova explosions [47] or neutron star cooling [48, 49]. In cosmology, the decay of relic axionic strings and domain walls produces a relevant cold dark matter population [50].

Still, besides new studies of red giant evolution — currently underway [51] — or features in massive star evolution such as [52] we know of no other way to test the WD cooling hypothesis that could rely *solely* on the axion-electron coupling. It appears thus that to assess the WD cooling hypothesis we must study processes involving other axion couplings as well. In this paper we will make use of the coupling to two photons. As already mentioned, the solar BCA flux of non-hadronic axions is generically much larger than that of hadronic models for the same value of  $f_a$  and moreover, it has a different spectrum (see figure 1).

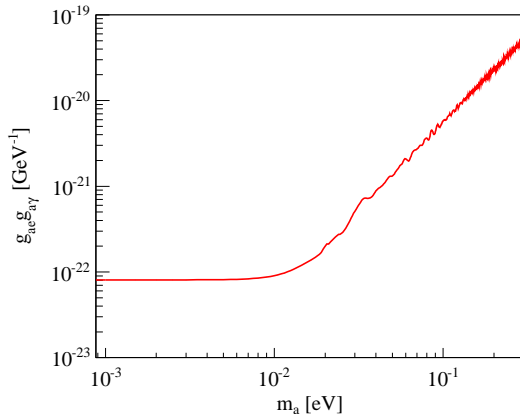


**Figure 2.** CAST constraints on  $g_{ae} \times g_{a\gamma}$  as a function of  $m_a$ , assuming the solar emission is dominated by the BCA reactions which involve only the electron coupling  $g_{ae}$ .

Therefore, helioscopes are appealing to search for non-hadronic axions. Indeed, some of us have recently shown that a next generation helioscope [53], such as the proposed International AXion Observatory (IAXO) [54] can test the WD cooling hypothesis down to very small couplings  $g_{ae} \sim 10^{-13}$ .

In the present paper we analyze the CAST data in search of non-hadronic axions and set new upper bounds on  $g_{ae} \times g_{a\gamma}$ , the product of the electron coupling (responsible for the production in the Sun) and the two-photon coupling (responsible for the detection in CAST).

Figure 2 shows our results when we assume that the Primakoff emission from the Sun is subdominant and therefore the solar flux is caused by the BCA reactions alone. Our analysis of CAST data then constrains

$$g_{a\gamma} \times g_{ae} < 8.1 \times 10^{-23} \text{ GeV}^{-1} \quad (95\% \text{ CL}) \quad (1.1)$$

at low masses  $m_a \lesssim 10$  meV — where the probability of axion-photon conversion in CAST becomes independent of the mass — and worsens as  $1/m_a^2$  for higher masses.

If we also include the Primakoff flux (which is unavoidable because it is produced by the same coupling  $g_{a\gamma}$  involved in the CAST detection), the signal at CAST depends independently on three parameters:  $g_{ae}$ ,  $g_{a\gamma}$  and  $m_a$ . However, for  $m_a \lesssim 10$  meV the detection is independent of mass and we can plot our results in the  $g_{ae}-g_{a\gamma}$  parameter space. In this low-mass range, phase-I of CAST gives the strongest constraints and thus we have focused only on this data set. Our analysis, based on a two-free parameter likelihood method is able to exclude the region above the thick black line in figure 3. For very small values of  $g_{ae} \lesssim 10^{-12}$ , the BCA flux is negligible and the CAST bound smoothly becomes  $g_{a\gamma} < 0.88 \times 10^{-10} \text{ GeV}^{-1}$  as found in our previous study [5] where only Primakoff emission was assumed. However, for larger values of  $g_{ae}$  the BCA flux becomes dominant and we recover equation 1.1.

Note that our bound relies on a simple calculation of the solar axion flux, for which we have taken a solar model unperturbed by axion emission. If  $g_{ae}$  or  $g_{a\gamma}$  are very large, the large axion flux requires a modified internal structure of the Sun with larger nuclear reaction rates and higher temperature of the core. The most stringent constraint derives from the agreement between the predicted and observed solar boron neutrino flux [55], excluding the gray region depicted in figure 3 (labeled Solar  $\nu$ ). Thus our bound is completely self-consistent up to  $g_{ae} = 3 \times 10^{-11}$ , in contrast to those solar axion searches utilising Bragg scattering [56–59]

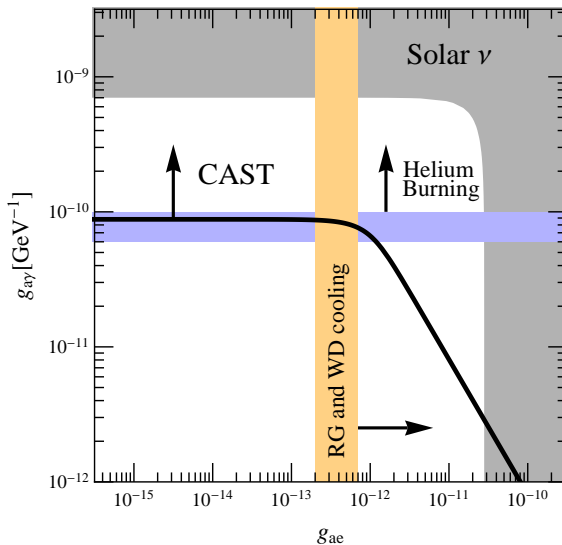


**Figure 3.** Constraints on  $g_{ae}$  and  $g_{a\gamma}$  for  $m_a \lesssim 10$  meV. The region above the thick black line is excluded by CAST. The gray region is excluded by solar neutrino measurements. In the vertical orange band, axion emission strongly affects white dwarf cooling and the evolution of low-mass red giants; parameters to the right of this band are excluded. Likewise, helium-burning stars would be perceptibly affected in the horizontal blue band; parameters above it are excluded.

which have more limited sensitivity [60], as well as to some other searches relying solely on  $g_{ae}$  coupling [61–63].

In order to put our results into context we also show in figure 3 two color bands representing parameters where axion emission would have a strong impact on stellar evolution. In the vertical orange band of  $g_{ae}$  values, axion emission would strongly affect WD cooling [37–44] and delay helium ignition in low-mass red giants [45, 46]. The exact range of  $g_{ae}$  values that is consistently ruled in or ruled out by these arguments remains to be studied in detail, but for sure parameters to the right of this band are excluded. Within the horizontal blue band, axion Primakoff emission would strongly affect stars in the helium-burning phase. The upper edge of this band corresponds to the traditional horizontal-branch star limit, the remaining range represents a new argument concerning the blue-loop suppression during the helium-burning phase of massive stars [52].

The orange band cuts the CAST constraint in its horizontal part which corresponds to the Primakoff flux dominating the solar flux, but very close to the values  $g_{ae} \sim 10^{-12}$  where the BCA flux starts to dominate. Therefore, CAST cannot shed any further light on the WD cooling hypothesis. However, a next-generation helioscope such as IAXO with its improved sensitivity to  $g_{a\gamma}$  will also benefit from the large BCA-emitted flux and will improve over the RG bound in part of the parameter space. In principle, the WD cooling hypothesis is then testable in a laboratory experiment.

After having presented our results and main messages, the rest of the paper is devoted to elaborate on our definitions, assumptions, and analysis method. In section 2 we give a brief account of axion theory, we further examine the implications of our findings, and finally describe the solar axion flux, and in section 4 we present our new analysis after a summary of the experimental setup of CAST phase-I and its results.

## 2 Properties of axions and axion-like particles

For the purpose of the present paper we can parametrize an axion model with the lagrangian density

$$\mathcal{L} = \frac{1}{2}(\partial_\mu a)(\partial^\mu a) - \frac{1}{2}m_a^2 a^2 - \frac{g_{a\gamma}}{4}F_{\mu\nu}\tilde{F}^{\mu\nu}a - g_{ae}\frac{\partial_\mu a}{2m_e}\bar{\psi}_e\gamma_5\gamma^\mu\psi_e, \quad (2.1)$$

where  $a$  is the axion field,  $m_a$  its mass,  $F_{\mu\nu}$  and  $\tilde{F}^{\mu\nu}$  are the electromagnetic field tensor and its dual,  $m_e$  the electron mass, and  $\psi_e$  the electron field. The coupling constant  $g_{a\gamma}$  has units of energy<sup>-1</sup> while  $g_{ae}$  is a dimensionless Yukawa coupling. Particles featuring this type of lagrangians are often called *axion-like particles* (ALPs) and they appear as pseudo-Nambu-Goldstone bosons (pNGB), associated with a global shift symmetry  $a \rightarrow a + \text{const.}$  which is spontaneously broken at some high energy scale  $f_a$  (sometimes called ALP decay constant) or stringy axions where  $f_a$  corresponds to the string scale  $M_s$ . The shift symmetry is explicitly broken by some perturbing dynamics responsible for the mass term.

In 1977 Peccei and Quinn proposed one such symmetry to solve the strong CP problem [64, 65] with the additional condition that it should be color anomalous. The resulting pNGB was called the axion [66, 67]. The axion receives its mass from chiral symmetry breaking after mixing with the pseudoscalar mesons through the color anomaly, its magnitude being

$$m_a = \frac{\sqrt{z}}{1+z} \frac{m_\pi f_\pi}{f_a} \simeq 6 \text{ meV} \frac{10^9 \text{ GeV}}{f_a}, \quad (2.2)$$

where  $m_\pi$  is the neutral pion mass and  $f_\pi$  is the pion decay constant. For the ratio  $z = m_u/m_d$  of up to down quark masses we use the canonical value  $z \sim 0.56$  although the allowed range is  $z = 0.35\text{--}0.60$  [68], however this only leads to minor uncertainties in our context.

The axion has a model-independent contribution to its two-photon coupling coming from the above-mentioned mixing with mesons and can also have a model-dependent part if the PQ symmetry has the electromagnetic anomaly. The two contributions sum to

$$g_{a\gamma} = \frac{\alpha}{2\pi f_a} \left( \frac{E}{N} - \frac{2}{3} \frac{4+z}{1+z} \right) \simeq \frac{\alpha}{2\pi f_a} \left( \frac{E}{N} - 1.92 \right), \quad (2.3)$$

where  $\alpha$  is the fine-structure constant and  $E/N$  the ratio of the electromagnetic and color anomalies of the PQ symmetry.

The coupling to electrons has a model-dependent contribution proportional to an  $O(1)$  coefficient  $X_e$  arising only in non-hadronic axion models and a very small model-independent one induced at one-loop via the photon coupling,

$$g_{ae} = X_e \frac{m_e}{f_a} + \frac{3\alpha^2}{4\pi} \frac{m_e}{f_a} \left( \frac{E}{N} \log \frac{f_a}{m_e} - 1.92 \log \frac{\Lambda}{m_e} \right), \quad (2.4)$$

where  $\Lambda$  is an energy scale close to the QCD confinement scale.

For a generic ALP,  $\phi$ , we expect similar equations for  $g_{\phi e}$  and  $g_{\phi\gamma}$  as for the axion, of course after removing the terms coming from axion-meson mixing, (the terms involving  $z$ ) and changing  $f_a$  for the ALP decay constant,  $f_\phi$ . However, the ALP mass is then completely unrelated to the couplings.

### 3 Expected counting rate

#### 3.1 Solar flux

Based on the different axion interactions, different processes contribute to the production of the solar flux of these particles (see figure 4). The most important processes are:

- Primakoff effect:  $\gamma + Q \rightarrow Q + a$
- Compton scattering (photo production):  $\gamma + e \rightarrow e + a$
- Electron-Ion bremsstrahlung (free-free transition):  $e + I \rightarrow e + I + a$
- Electron-electron bremsstrahlung:  $e + e \rightarrow e + e + a$
- Axio-recombination (free-bound transition):  $e + I \rightarrow I^- + a$
- Axio-deexcitation (bound-bound transition):  $I^* \rightarrow I + a$

where  $Q$  stands for any charged particle in the solar plasma,  $e$  for electrons,  $I$  for ions and  $I^*$  for their excited states. The Primakoff process depends on the two-photon coupling and dominates when the coupling to electrons is absent at tree-level. When this is not the case the BCA processes dominate: bremsstrahlung on hydrogen and helium nuclei dominates the emission of low-energy axions, axio-recombination of metals (mostly O, Ne, Si, S and Fe) contributes sizably at intermediate energies and Compton takes over at higher energies. The contribution of axio-deexcitation is dominated by Lyman transitions (mostly Ly- $\alpha$ ) and is significant only in the case of iron which dominates the axion flux around  $\sim 6.5$  keV. Following Ref. [15] and integrating the emission rates over a solar model [69], the following

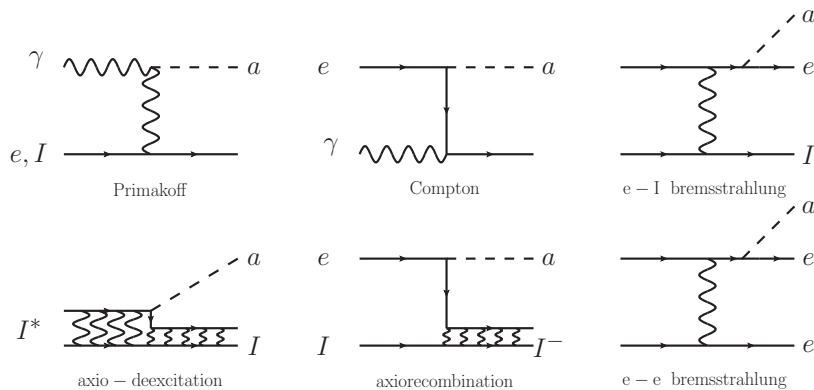


**Figure 4.** Some Feynman diagrams for the most relevant solar axion emission reactions included in this work.

fits for the axion fluxes at Earth can be obtained [53] (in units of  $\text{m}^{-2} \text{year}^{-1} \text{keV}^{-1}$ )

$$\left. \frac{d\Phi_a}{d\omega} \right|_P = 2.0 \times 10^{18} \left( \frac{g_{a\gamma}}{10^{-12} \text{GeV}^{-1}} \right)^2 \omega^{2.450} e^{-0.829 \omega} \quad (3.1)$$

$$\left. \frac{d\Phi_a}{d\omega} \right|_C = 4.2 \times 10^{18} \left( \frac{g_{ae}}{10^{-13}} \right)^2 \omega^{2.987} e^{-0.776 \omega} \quad (3.2)$$

$$\left. \frac{d\Phi_a}{d\omega} \right|_B = 8.3 \times 10^{20} \left( \frac{g_{ae}}{10^{-13}} \right)^2 \frac{\omega}{1 + 0.667 \omega^{1.278}} e^{-0.77 \omega} \quad (3.3)$$



where  $\omega$  is the axion energy in keV, while P, C and B stand for Primakoff, Compton, and bremsstrahlung, respectively. In particular, the bremsstrahlung flux includes both electron-nucleus (only H and He) and electron-electron contributions. As a novelty, we include the emission of axions in the electron capture by an ion, dubbed “axio-recombination” (free-bound transition) and atomic “axio-deexcitation” (bound-bound transition). Originally, the former process was estimated to be subdominant in the Sun [34, 35]. However, a new calculation to be presented elsewhere [30], including the missing factor of 2 in the cross-section pointed out in [36] and captures in higher shells than the K-shell, shows that these processes are significant and increase the total flux by a factor of order 1 (figure 1). Unfortunately, the kinematic edges and the narrow lines from bound-bound transitions prevent us from providing a simple fitting formula.

### 3.2 Helioscope event number

The expected number of photons  $\mathcal{N}_\gamma$  from axion conversion in a given detector is obtained by integrating the product of the differential axion flux, conversion probability and detection efficiency over the total range of energies

$$\mathcal{N}_\gamma = \int_{\omega_0}^{\omega_f} d\omega \left( \frac{d\Phi_a}{d\omega} \right)_{\text{total}} \mathcal{P}_{a \rightarrow \gamma} \epsilon S t \quad (3.4)$$

where  $S$  is the detection area perpendicular to the flux of axions,  $t$  is the exposure time, and  $\epsilon$  the detection efficiency. The axion-photon conversion probability in a transverse homogeneous magnetic field  $B$  over distance  $L$  is

$$\mathcal{P}_{a \rightarrow \gamma} = \left( \frac{g_{a\gamma} B L}{2} \right)^2 \text{sinc}^2 \left( \frac{qL}{2} \right), \quad (3.5)$$

where  $\text{sinc } x = (\sin x)/x$  and the momentum transfer provided by the magnetic field is  $q = m_a^2/2\omega$ . Coherent  $a$ - $\gamma$  conversion along the full magnetic length happens when  $m_a^2 < 4\omega/L$ , i.e. when the momentum transfer is smaller than about  $1/L$ , where  $\text{sinc}(qL/2) \rightarrow 1$ . For larger masses, the conversion is not coherent<sup>2</sup> and the probability gets suppressed by a factor  $\sim (4\omega/m_a^2 L)^2$ . This factor is responsible for the degradation of our bound for  $m_a \gtrsim 10$  meV seen in figure 2.

## 4 CAST experiment and analysis

The most sensitive helioscope to date is the CERN Axion Solar Telescope (CAST), which makes use of a prototype superconducting LHC dipole magnet providing a magnetic field of up to 9 T. CAST is able to follow the Sun twice a day during sunrise and sunset for a total of 3 h per day. At both ends of the 9.26 m long magnet, X-ray detectors [70–72] have been mounted to search for photons from Primakoff conversion.

CAST began its operation in 2003 and, after two years of data taking, determined an upper limit on  $g_{a\gamma} \lesssim 0.88 \times 10^{-10} \text{ GeV}^{-1}$  at 95 % CL for  $m_a \leq 0.02$  eV [4, 5] in the hadronic axion scenario. To extend the experimental sensitivity to larger axion masses, the conversion region of CAST was filled with a suitable buffer gas [73] providing the photons with an effective mass, yielding upper limits on  $g_{a\gamma} \lesssim 2.3 \times 10^{-10} \text{ GeV}^{-1}$  for  $0.02 \leq m_a \leq 0.65$  eV [6, 7]. Higher axion masses have also been studied and future publications will report on these masses which cover a range up to 1.18 eV.

<sup>2</sup>We only use data from the CAST vacuum phase where photon refraction by the residual gas can be neglected due to the high vacuum conditions [5].

## 4.1 The X-ray telescope of CAST

The most sensitive detector system operative at CAST phase-I was the X-ray telescope [72], a combination of X-ray mirror optics [74] and a Charge-Coupled Device (CCD) [75] located in the focal plane of the mirror optics. Both instruments were originally built for satellite space missions, and together they increase the axion discovery potential significantly along with providing excellent imaging capability. The implementation of the X-ray mirror optics suppresses background by a factor of  $\sim 155$ , since photons are focused from the magnet aperture area of about  $14.5\text{ cm}^2$  to a spot of roughly  $9.3\text{ mm}^2$  on the CCD chip. One of the resulting advantages of focusing optics is the possibility to measure background and signal simultaneously.

## 4.2 Data taking

The CCD detector showed a stable performance over the entire 2004 running period. For our analysis, we have used a total of 197 h of tracking data (i.e. magnet pointing to the Sun) and 1890 h of background data taken from the same area during non-tracking periods. For a detailed description of the X-ray telescope design, its performance, and background systematics during the 2004 data taking period we refer to Ref. [70]. Since no significant signal over background was detected with the X-ray telescope during the data taking period of 2004, upper limits for the non-hadronic axions were derived for this CAST detector system.

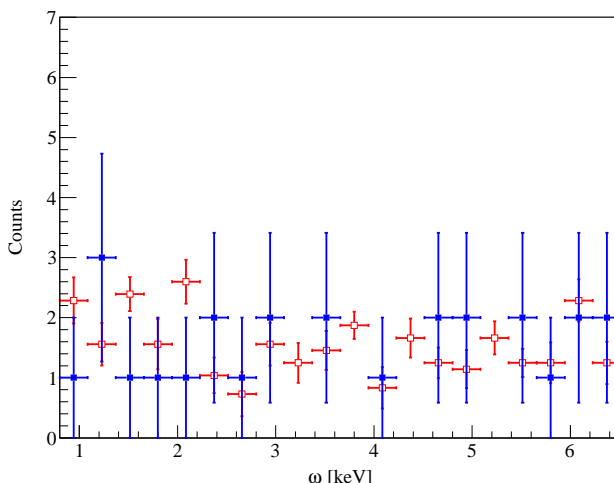


**Figure 5.** CCD spectra for tracking (blue) and background (red) runs during 2004. In both cases, the error bars represent the statistical uncertainty of the measurement. Please notice that the background spectrum has been renormalized to the tracking time of 197 hours.

In order to minimize the influence of the  $\text{Cu-K}_\alpha$  fluorescence line (at 8 keV originating from the cooling mask of the detector [70]), we restricted our analysis to the energy range between 0.8 and 6.8 keV. In total, we observe 26 counts in this energy range inside the signal-spot area during axion sensitive conditions. The background, defined by the data taken from the same CCD spot region during non-tracking periods, has been acquired under the same operating conditions. The spectral distribution of the observed events during tracking and non-tracking times with the CCD detector is shown in figure 5.

### 4.3 Spectral fitting results

The resulting low counting statistics required the use of a maximum-likelihood method to determine an upper limit on  $g_{ae}^2 g_{a\gamma}^2$ . The likelihood function used is based on a Poissonian p.d.f., the binned likelihood

$$\mathcal{L} = \prod_j^n \frac{e^{-\lambda_j} \lambda_j^{t_j}}{t_j!}, \quad (4.1)$$

where  $n = 20$  is the number of spectral bins,  $t_j$  the number of observed counts in tracking, and  $\lambda_j$  the value of the mean in the  $j$ -th bin, respectively. The fit function,  $\lambda_j = \sigma_j + b_j$  is used, where  $b_j$  is the measured background and  $\sigma_j \propto g_{ae}^2 g_{a\gamma}^2$  is the expected number of counts in the  $j^{\text{th}}$  energy bin from axion-to-photon conversion. The best estimate for  $g_{ae}^2 g_{a\gamma}^2$  is obtained by minimizing  $\chi^2 = -2 \ln \mathcal{L}$ . The validity of the  $\chi^2$ -interpretation in our case, as well as the negligible influence of the statistical uncertainty of the background on the final result have been verified with a Monte Carlo model by means of the generation of pseudo-data sets.

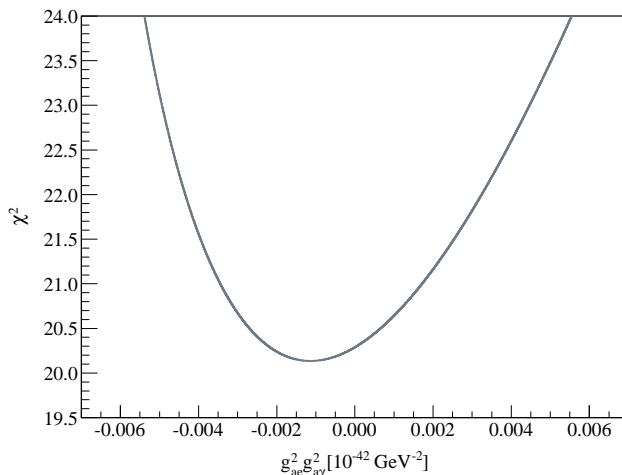


**Figure 6.**  $\chi^2$  as function of  $g_{ae}^2 g_{a\gamma}^2$  for an axion mass of 1 meV. The minimum of the  $\chi^2$  distribution,  $-1.136 \times 10^{-45} \text{ GeV}^{-2}$ , is the most probable value of  $g_{ae}^2 g_{a\gamma}^2$ .

We compared the result derived with the maximum-likelihood defined in equation 4.1 with a maximum-likelihood technique based on an unbinned maximum-likelihood estimator that divides the exposure time in sufficiently small time fragments so that either one or zero counts are found in the detector. The unbinned likelihood can be expressed as

$$\log \mathcal{L} \propto -R_T + \sum_k^N \log R(t_k, \omega_k) \quad (4.2)$$

where the sum runs over each of the  $N$  detected counts and  $R(t_k, \omega_k)$  is the event rate at the time  $t_k$ , energy  $\omega_K$  of the  $k$ -event.  $R_T$  is the expected number of counts over all exposure time and energy

$$R(t, \omega) = B + S(t, \omega) \quad (4.3)$$

where  $B$  is the background rate of the detector and  $S(t, \omega)$  is the expected rate from axions ( $\mathcal{N}_\gamma$ ), which depends on the axion properties  $g_{a\gamma}$  and  $m_a$  (see equation 3.4).

The final analysis yields an upper limit on  $g_{ae}g_{a\gamma} \lesssim 8.1 \times 10^{-23} \text{ GeV}^{-1}$  (95% CL) for axion masses  $m_a \leq 10 \text{ meV}$  (see figure 2). Both likelihood methods give compatible results on both, the best fit value and the upper limit. In the latter case the deviation of the limit remains within  $\sim 0.3\%$  over the considered axion mass range.

Parallel to the methods described above, a two-free parameter likelihood was applied for axion masses within the reach of CAST. In this case, not only is the axion-electron coupling taken into account but also the Primakoff contribution to the axion production in the Sun in the frame of non-hadronic models. This approach computes a three-dimensional probability function at a given axion mass that correlates both  $g_{a\gamma}$  and  $g_{ae}$  couplings. The result yields a limit on the  $g_{a\gamma}$ - $g_{ae}$  parameter space (see figure 3).

#### 4.4 Systematic uncertainties

We studied the influence of systematic uncertainties on the best fit value of  $g_{ae}^2 g_{a\gamma}^2$  and on the upper limit. Statistically significant variations of the background on long and short time scales are not apparent for the X-ray telescope data [70]. Even if the background level were time-dependent, it would not play a significant role, since the X-ray telescope is measuring both, potential signal and background, simultaneously. Since we observed no significant difference between the background level and the spatial distribution during tracking and non-tracking times, we used the same signal-spot area during non-tracking periods to define the background. Alternatively, we used tracking data and different regions on the CCD outside the signal spot area to estimate the systematic uncertainties due to the choice of background definition. The overall systematic uncertainty is dominated by both the background definition and the pointing accuracy, that affects the effective area of the telescope, the location of the signal spot and its size, respectively. Other effects such as uncertainties in the detector calibration, magnet parameters and the likelihood method used are negligible in comparison with the systematic induced by the choice of background definition. For the best fit value of  $g_{ae}^2 g_{a\gamma}^2$  we find that in the axion mass range for which CAST remains coherent we obtain

$$g_{ae}^2 g_{a\gamma}^2 |_{\text{bestfit}} = (-1.136 \pm_{2.46}^{3.09} \text{ stat.} \pm_{2.24}^{2.20} \text{ syst.}) \times 10^{-45} \text{ GeV}^{-2}. \quad (4.4)$$

Alternatively, the background was also determined by extrapolating the background measured during tracking periods in the part of the CCD not containing the Sun spot. Different background selections led to different upper limits on  $g_{ae}^2 g_{a\gamma}^2$ , all of them within the statistical uncertainty.

## 5 Conclusions

Axions with tree-level coupling to electrons provide a different physics case and phenomenology than hadronic models. From the theoretical point of view, non-hadronic models are appealing because they arise in grand unified theories (GUTs), well-motivated completions of the standard model at high energies. From the phenomenological side, it is worth noting that naturally the coupling to electrons leads to larger axion fluxes from stars than the coupling to photons. The sensitivity of CAST to non-hadronic axions allows us to set a bound on the product of both coupling constants  $g_{ae}g_{a\gamma} \lesssim 8.1 \times 10^{-23} \text{ GeV}^{-1}$  for  $m_a \leq 10 \text{ meV}$ .

For hadronic axions, Primakoff emission is the dominant production process in stars and helioscope limits depend only on the axion-photon interaction strength  $g_{a\gamma}$ . For low-mass axions, the CAST limit on  $g_{a\gamma}$  is competitive with, and even somewhat superior to, the energy-loss limits from globular cluster stars. For non-hadronic models, the stellar fluxes are dominated by the BCA processes that are based on the axion-electron coupling  $g_{ae}$ . In this case CAST constrains the product  $g_{ae}g_{a\gamma}$  in a significant way. However, the stellar energy-loss limits on  $g_{ae}$  are so restrictive here that CAST is not yet competitive.

The claim of an anomalous energy loss in white dwarfs could be an indication for the existence of axions with a coupling to electrons in the  $g_{ae} \sim 10^{-13}$  range, close to the energy-loss limits of red giants in globular clusters. If we are to assume this hint, the flux of solar axions is fixed by this parameter and a next generation axion helioscope such as IAXO could be able to detect it. We believe that the test of the white-dwarf claim and surveying the DFSZ parameter space for the first time in a laboratory experiment is a compelling motivation for IAXO and strengthens its physics case.

In summary, there is a strong motivation to improve the helioscope sensitivity beyond CAST down to  $g_{a\gamma} \sim 10^{-12} \text{ GeV}^{-1}$  and  $g_{ae} \sim 10^{-13}$  [53]. This region includes, on the high-mass end, a large set of favored QCD axion models, potentially supersedes limits from SN 1987A and red giants in non-hadronic models, and starts probing the parameters suggested by white-dwarf cooling.

## Acknowledgments

We thank CERN for hosting the experiment. This article has been authored by Lawrence Livermore National Security, LLC under Contract No. DE-AC52-07NA27344 with the U.S. Department of Energy. Accordingly, the United States Government retains and the publisher, by accepting the article for publication, acknowledges that the United States Government retains a non-exclusive, paid-up, irrevocable, world-wide license to publish or reproduce the published form of this article or allow others to do so, for United States Government purposes. We acknowledge support from NSERC (Canada), MSES (Croatia) under Grant No. 098-0982887-2872, CEA (France), BMBF (Germany) under Grant Nos. 05 CC2EEA/9 and 05 CC1RD1/0, DFG (Germany) under Grant Nos. HO 1400/7-1 and EXC-153, VIDMAN (Germany), GSRT (Greece), RFFR (Russia), the Spanish Ministry of Economy and Competitiveness (MINECO) under Grant Nos. FPA2007-62833 and FPA2008-03456, NSF (USA) under Award No. 0239812, NASA under Grant No. NAG5-10842, and the European Union under Grant No. PITN-GA-2011-289442 (ITN “Invisibles”). J. Redondo acknowledges support by the Alexander von Humboldt Foundation.

## References

- [1] K. Zioutas, *et al.*, Nucl. Instrum. Meth. A **425** (1999) 480 [astro-ph/9801176].
- [2] P. Sikivie, Phys. Rev. Lett. **51** (1983) 1415; (E) *ibid.* **52** (1984) 695.
- [3] G. Raffelt and L. Stodolsky, Phys. Rev. D **37**, (1988) 1237.
- [4] K. Zioutas *et al.* [CAST Collaboration], Phys. Rev. Lett. **94** (2005) 121301 [hep-ex/0411033].
- [5] S. Andriamonje *et al.* [CAST Collaboration], JCAP **0704** (2007) 010 [hep-ex/0702006].
- [6] E. Arik *et al.* [CAST Collaboration], JCAP **0902** (2009) 008 [arXiv:0810.4482].
- [7] M. Arik *et al.* [CAST Collaboration], Phys. Rev. Lett. **107** (2011) 261302 [arXiv:1106.3919].

- [8] S. Andriamonje *et al.* [CAST Collaboration], JCAP **1003** (2010) 032 [arXiv:0904.2103].
- [9] S. Andriamonje *et al.* [CAST Collaboration], JCAP **0912** (2009) 002 [arXiv:0906.4488].
- [10] J. E. Kim, Phys. Rev. Lett. **43** (1979) 103.
- [11] M. A. Shifman, A. I. Vainshtein and V. I. Zakharov, Nucl. Phys. B **166** (1980) 493.
- [12] T. Moroi and H. Murayama, Phys. Lett. B **440** (1998) 69 [hep-ph/9804291].
- [13] M. Srednicki, Nucl. Phys. B **260** (1985) 689.
- [14] D. A. Dicus, E. W. Kolb, V. L. Teplitz and R. V. Wagoner, Phys. Rev. D **18** (1978) 1829.
- [15] G. G. Raffelt, Phys. Rev. D **33** (1986) 897.
- [16] G. G. Raffelt, Phys. Rev. D **37** (1988) 1356.
- [17] P. Svrcek and E. Witten, JHEP **0606** (2006) 051 [hep-th/0605206].
- [18] A. Arvanitaki, S. Dimopoulos, S. Dubovsky, N. Kaloper and J. March-Russell, Phys. Rev. D **81** (2010) 123530 [arXiv:0905.4720].
- [19] B. S. Acharya, K. Bobkov and P. Kumar, JHEP **1011** (2010) 105 [arXiv:1004.5138].
- [20] G. F. Giudice, R. Rattazzi and A. Strumia, Phys. Lett. B **715** (2012) 142 [arXiv:1204.5465].
- [21] M. Cicoli, M. Goodsell, A. Ringwald, M. Goodsell and A. Ringwald, JHEP **1210** (2012) 146 [arXiv:1206.0819].
- [22] M. Redi and A. Strumia, JHEP **1211** (2012) 103 [arXiv:1208.6013].
- [23] A. Ringwald, Phys. Dark Univ. **1** (2012) 116 [arXiv:1210.5081].
- [24] J. Jaeckel, M. Jankowiak and M. Spannowsky, arXiv:1212.3620.
- [25] M. P. Hertzberg, arXiv:1210.3624.
- [26] A. Chatzistavrakidis, E. Erfani, H. P. Nilles and I. Zavala, JCAP **1209** (2012) 006 [arXiv:1207.1128].
- [27] R. D. Peccei, Lect. Notes Phys. **741** (2008) 3 [hep-ph/0607268].
- [28] A. R. Zhitnitsky, Sov. J. Nucl. Phys. **31** (1980) 260 [Yad. Fiz. **31** (1980) 497].
- [29] M. Dine, W. Fischler and M. Srednicki, Phys. Lett. B **104** (1981) 199.
- [30] J. Redondo, in preparation.
- [31] L. M. Krauss, J. E. Moody and F. Wilczek, Phys. Lett. B **144** (1984) 391.
- [32] M. Fukugita, S. Watamura and M. Yoshimura, Phys. Rev. Lett. **48** (1982) 1522.
- [33] M. Fukugita, S. Watamura and M. Yoshimura, Phys. Rev. D **26** (1982) 1840.
- [34] S. Dimopoulos, J. A. Frieman, B. W. Lynn and G. D. Starkman, Phys. Lett. B **179** (1986) 223.
- [35] S. Dimopoulos, G. D. Starkman and B. W. Lynn, Mod. Phys. Lett. A **1** (1986) 491.
- [36] A. Derevianko, V. A. Dzuba, V. V. Flambaum and M. Pospelov, Phys. Rev. D **82** (2010) 065006 [arXiv:1007.1833].
- [37] J. Isern, M. Hernanz and E. García-Berro Astrophys. J. **392**, L23 (1992).
- [38] J. Isern, E. García-Berro, L. G. Althaus and A. H. Córscico, Astron. Astrophys. **512**, A86 (2010) [arXiv:1001.5248].
- [39] A. H. Córscico, L. G. Althaus, M. M. M. Bertolami, A. D. Romero, E. García-Berro, J. Isern and S. O. Kepler, Mon. Not. R. Astron. Soc. **424** (2012) 2792 [arXiv:1205.6180].
- [40] A. H. Córscico, L. G. Althaus, A. D. Romero, A. S. Mukadam, E. García-Berro, J. Isern, S. O. Kepler and M. A. Corti, JCAP **1212** (2012) 010 [arXiv:1211.3389].

- [41] J. Isern, E. García-Berro, S. Torres and S. Catalán, *Astrophys. J. Lett.* **682** (2008) L109 [arXiv:0806.2807].
- [42] J. Isern, S. Catalán, E. García-Berro and S. Torres, *J. Phys. Conf. Ser.* **172** (2009) 012005 [arXiv:0812.3043].
- [43] J. Isern, L. Althaus, S. Catalán, A. Córscico, E. García-Berro, M. Salaris and S. Torres, arXiv:1204.3565.
- [44] B. Melendez, M. M. Bertolami and L. Althaus, arXiv:1210.0263.
- [45] G. G. Raffelt, *Astrophys. J.* **365** (1990) 559.
- [46] G. Raffelt and A. Weiss, *Phys. Rev. D* **51** (1995) 1495 [hep-ph/9410205].
- [47] G. G. Raffelt, J. Redondo and N. Viaux Maira, *Phys. Rev. D* **84** (2011) 103008 [arXiv:1110.6397].
- [48] H. Umeda, N. Iwamoto, S. Tsuruta, L. Qin and K. Nomoto, astro-ph/9806337.
- [49] J. Keller and A. Sedrakian, *Nucl. Phys. A* **897**, (2013) 62 [arXiv:1205.6940].
- [50] T. Hiramatsu, M. Kawasaki, K. Saikawa and T. Sekiguchi, *Phys. Rev. D* **85** (2012) 105020 [arXiv:1202.5851].
- [51] N. Viaux, M. Catelan, P. B. Stetson, G. G. Raffelt, J. Redondo and A. A. R. Valcarce, work in progress (2013).
- [52] A. Friedland, M. Giannotti and M. Wise, *Phys. Rev. Lett.* **110** (2013) 061101 [arXiv:1210.1271].
- [53] I. G. Irastorza *et al.*, *JCAP* **1106** (2011) 013 [arXiv:1103.5334].
- [54] I. G. Irastorza *et al.* [IAXO Collaboration], *EAS Publication Series* **53**, (2011) 147 [arXiv:1201.3849].
- [55] P. Gondolo and G. Raffelt, *Phys. Rev. D* **79** (2009) 107301 [arXiv:0807.2926].
- [56] F. T. Avignone, III *et al.* [SOLAX Collaboration], *Phys. Rev. Lett.* **81** (1998) 5068 [astro-ph/9708008].
- [57] A. Morales *et al.* [COSME Collaboration], *Astropart. Phys.* **16** (2002) 325 [hep-ex/0101037].
- [58] R. Bernabei *et al.*, *Phys. Lett. B* **515** (2001) 6.
- [59] Z. Ahmed *et al.* [CDMS Collaboration], *Phys. Rev. Lett.* **103** (2009) 141802 [arXiv:0902.4693].
- [60] S. Cebrián *et al.*, *Astropart. Phys.* **10** (1999) 397 [astro-ph/9811359].
- [61] D. Kekez, A. Ljubicic, Z. Krecak and M. Krmar, *Phys. Lett. B* **671** (2009) 345 [hep-ex/0807.3482].
- [62] A. V. Derbin, I. S. Drachnev, A. S. Kayunov and V. N. Muratova, *JETP Lett.* **95** (2012) 379 [hep-ex/1206.4142].
- [63] K. Abe *et al.*, astro-ph/1212.6153.
- [64] R. D. Peccei and H. R. Quinn, *Phys. Rev. Lett.* **38** (1977) 1440.
- [65] R. D. Peccei and H. R. Quinn, *Phys. Rev. D* **16** (1977) 1791.
- [66] S. Weinberg, *Phys. Rev. Lett.* **40** (1978) 223.
- [67] F. Wilczek, *Phys. Rev. Lett.* **40** (1978) 279.
- [68] K. Nakamura *et al.* [Particle Data Group], *J. Phys. G.* **37** (2010) 075021.
- [69] S. Turck-Chièze *et al.*, *Astrophys. J.* **555** (2001) L69.
- [70] M. Kuster *et al.*, *New J. Phys.* **9** (2007) 169 [physics/0702188].
- [71] P. Abbon *et al.*, *New J. Phys.* **9** (2007) 170 [physics/0702190].

- [72] D. Autiero *et al.*, New J. Phys. **9** (2007) 171 [physics/0702189].
- [73] K. van Bibber, P. M. McIntyre, D. E. Morris and G. G. Raffelt, Phys. Rev. D **39** (1989) 2089.
- [74] P. Friedrich *et al.*, Proc. SPIE **3444** (1998) 342.
- [75] L. Strüder *et al.*, Nucl. Instrum. Meth. A **454** (2000) 73.